Bull. Fac. Fish. Hokkaido Univ.
39(2), 96-105. 1988.

On Similarity of Eddy Area behind Simplified Components in Artificial Reef Structure

Cheng-Hai WANG*, Osamu SATO*, Katsuaki NASHIMOTO*
and Katsutaro YAMAMOTO*

Abstract

The properties of the eddy area behind the square prisms with widths of 4.0, 6.0, 8.0, 10.0 cm were investigated in a large-scale water channel. The similarity of the eddy areas was analyzed by the relationship of the drag of the model and the strength of the eddy under conditions of both the variable flow speeds with the same Reynolds number and varying Reynolds numbers with the same flow speed. The root mean square value of the sideward pressure of eddy, which was obtained by a strain gage sensor set perpendicularly to the flow direction, was defined as a parameter P_{RMS}, representing the strength of eddy. The distributions of the P_{RMS} under the different Reynolds numbers with the same flow speed were similar; the ones under the same Reynolds number could be similarily expressed by a parameter P_{RMS}/f, where f is the unchangeable dominant frequency of eddy. And within the Reynolds number range of $1.0\times10^4\sim2.5\times10^4$ used in this experiment, the distributions of the strength of eddy could be expressed similarly by a non-dimensional parameter CP_{RMS}, i.e. the value of $2P_{RMS}/\rho U^2$, where ρ is the density of water and U the speed of steady flow. Results indicate that the artificial reef structures can be designed to more economically and effectively generate and utilize the eddy.

Introduction

Artificial reefs successfully aggregate fishes. The eddy generated by these reefs is assumed to play an important role in fish aggregation (Artificial Reef Comprehensive Research Association, 1976; Bohnsack, et al., 1985). At present, there are over one hundred kinds of artificial reef structures in use, but the properties of the eddy areas generated by them are almost unknown. Several studies of eddies have been carried out using the different methods: using a dye or tracer to visualize the flow pattern around models of artificial reef structures (Sato, 1977; Kageyama et al., 1980); using a current meter to measure the flow speed and compare the distribution patterns of the velocity (Sakuda et al., 1981; Sakuda et al., 1982; Matsumi et al., 1985); assuming the flow to be a kind of potential flow and using a discrete vortex approximation for the free shear layers to simulate the vortices shedding behind a model of the artificial reef structure (Sawaragi et al., 1981; Sawaragi et al., 1984). There are, however, few papers utilizing the power spectrum to analyze the hydrodynamic characteristics of the eddy generated by the components in artificial reef structures. The flow speed around reef structures usually changes with the environmental conditions in the field, and the shape and size of the components are also variable. Knowledge of the eddy area behind the components will be very

* *Laboratory of Fishing Gear Engineering, Faculty of Fisheries, Hokkaido University*
(北海道大学水産学部漁具設計学講座)

useful for optimizing the design of artificial reef structures. In a previous paper, the basic hydrodynamic characteristics, i.e., the relationships between the frequency and the sideward pressure of eddies of different shape and size at different flow speeds, were reported (Wang, et al., 1986). In this paper, the similarity of eddy areas was investigated under the same and different Reynolds numbers.

Materials and Methods

The square prism, which had a greater eddy strength than the triangular prism, quadranglar prism and cylinder also used in the previous experiment, was chosen as a representative model for this experiment. The experiment was carried out in a large-scale water channel with the test section being 6 m×2 m×1 m. The sideward pressure of eddy was measured by a strain gage sensor set perpendicularly to the direction of the steady flow. The analog data were obtained through the A/D conversion system and were analyzed by computer. The details of the measuring system and models were described in the previous paper (Wang, et al., 1986). The experiment was carried out in two steps: firstly, the Reynolds number was kept constant at 1.5×10^4, but different models of size 4.0, 6.0, 8.0 and 10.0 cm, with corresponding flow speeds of 45, 30, 22.5 and 18 cm/sec respectively, were employed; secondly, the Reynolds number was varied from 1.0×10^4 to 2.5×10^4, but the flow speed was maintained at 30 cm/sec.

The sideward pressure of eddy was measured by the sensor at two series of measuring points along the distances A/a and B/a, where A is the backward distance from the downstream side of the model to the measuring point on the geometrically central line, B the sideward distance from the central line to the measuring point, and a the width of the model. The sideward pressure of eddy was measured along two series of points until the dominant frequency became unstable. The measured range was within $A/a=44$ and $B/a=6$, the sampling frequency was 10 or 20 Hz, and the sampling time was 25.6 or 12.8 seconds for the stable analog data of the sideward pressure of eddy. The analog data were calculated in the root mean square values in order to represent the strength of the fluctuation of the sideward pressure of eddy. The dominant frequency of eddy was examined by the power spectrum, which was obtained from analog data through the FFT algorithm. The eddy areas were compared by means of the distributions of the root mean square values and the dominant frequencies.

The eddy area may be considered from the point of view of the drag of the model, because the eddy area is created by the model and the drag is caused by the transformation of the steady flow into the eddy. Here, it was assumed that the energy of the eddy is correlated with the drag of the model for the purposes of analyzing the properties of the eddy area.

Generally, the drag of model can be expressed as:

$$D=\frac{1}{2}C_D\rho SU^2 \tag{1}$$

where C_D is the drag coefficient, ρ the density of water, S the projected area, and U the speed of the steady flow. The pressure on the front surface of model can be expressed as:

$$P=\frac{1}{2}\ C_D\rho U^2 \tag{2}$$

Equation (2) can be also expressed as:

$$P=\frac{1}{2}\ C_D\rho\ (aU)\left(\frac{U}{a}\right) \tag{3}$$

where a is the width of the models.

The Strouhal number can be expressed as:

$$S_t=\frac{fa}{U} \tag{4}$$

where f is the dominant frequency of eddy, and S_t is a constant for the model of the same shape (Wang, et al., 1986). If the Reynolds numbers are the same, in terms of Equation (4) and Equation (3) a constant can be expressed as:

$$C_1=\frac{1}{2}\ \frac{C_D\rho\ (aU)}{S_t} \tag{5}$$

Therefore, the P and f can expressed as:

$$\frac{P}{f}=C_1 \tag{6}$$

in all cases.

On the other hand, for the same flow speed, based on Equation (2), a constant can be expressed as:

$$C_2=\frac{1}{2}\ C_D\rho U^2 \tag{7}$$

and the pressure as:

$$P=C_2 \tag{8}$$

If the root mean square value of the sideward pressure of eddy is proportional to the pressure on the model, and the development and attenuation of the eddy is similar in the flow field, then Equation (6) and (8) can be verified by experimental means. Furthermore, because the drag coefficient and Strouhal number remain almost constant within a certain range of Reynolds numbers, therefore, the eddy area for different Reynolds numbers can be expressed similarly by a non-dimensional parameter CP_{RMS}, defined as:

$$CP_{RMS}=\frac{P_{RMS}}{\frac{1}{2}\ \rho U^2} \tag{9}$$

where P_{RMS} is the root mean square value of the measured sideward pressure of eddy.

Results

The power spectra at the measuring points along the central line ($B/a=0$), are shown in Fig. 1(a-d) for the models under the same Reynolds number of 1.5×10^4. Fig. 2(a-d) shows the power spectra along the side areas ($A/a=5$). From the power spectra it was found that the dominant frequency of the eddies was unchangeable within a certain range of A/a and B/a for the combination of model size and flow speed. The sideward range of this eddy area was the same about 5 times the model

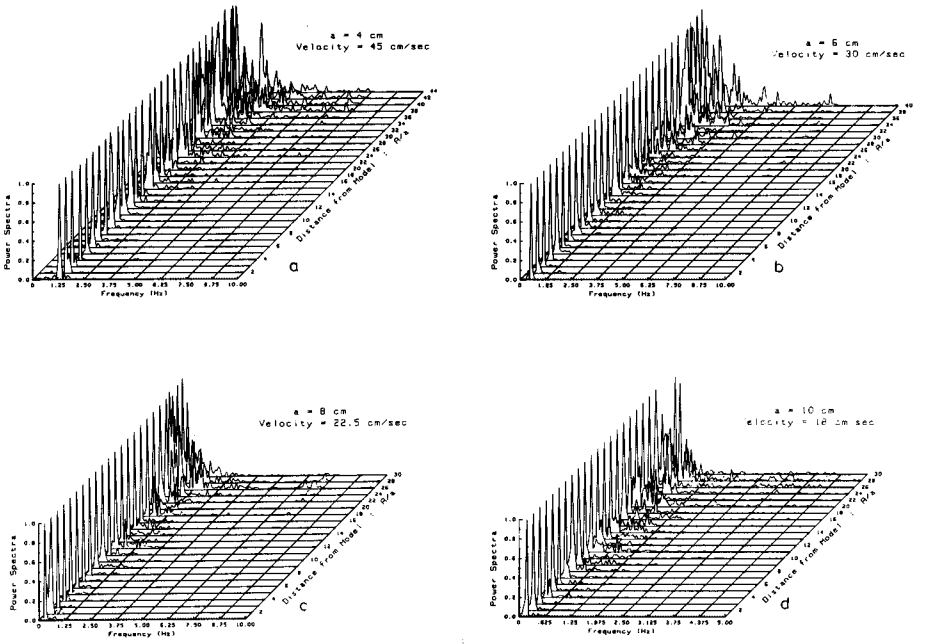

Fig. 1(a-d). The dominant freqency of eddies along the central line ($B/a=0$) under the same Reynolds number 1.5×10^4.

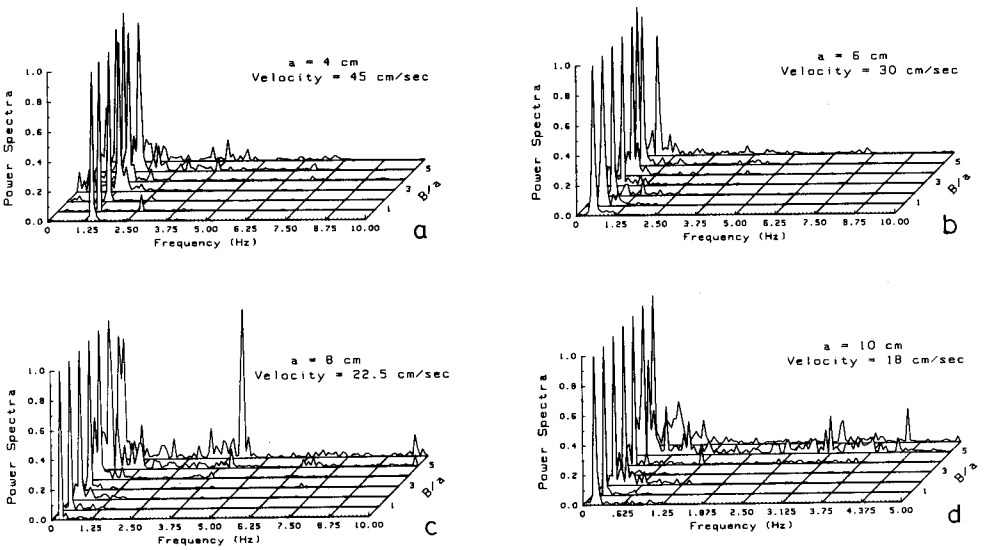

Fig. 2(a-d). The dominant freqency of eddies along the cross line ($A/a=5$) under the same Reynolds number 1.5×10^4.

size, the backward distance A/a was about 36 times the model size for the model of 4.0 cm, 32 for 6.0 cm, 26 for 8.0 cm and 24 for 10.0 cm. The stable dominant frequency was also different and the value was 1.33 Hz for the model of 4.0 cm, 0.55 Hz for 6.0 cm, 0.31 Hz for 8.0 cm and 0.20 Hz for 10.0 cm.

The distributions of the parameter P_{RMS}/f along the central line and side area are shown in Fig. 3 and Fig. 4 respectively. The results show that the distributions

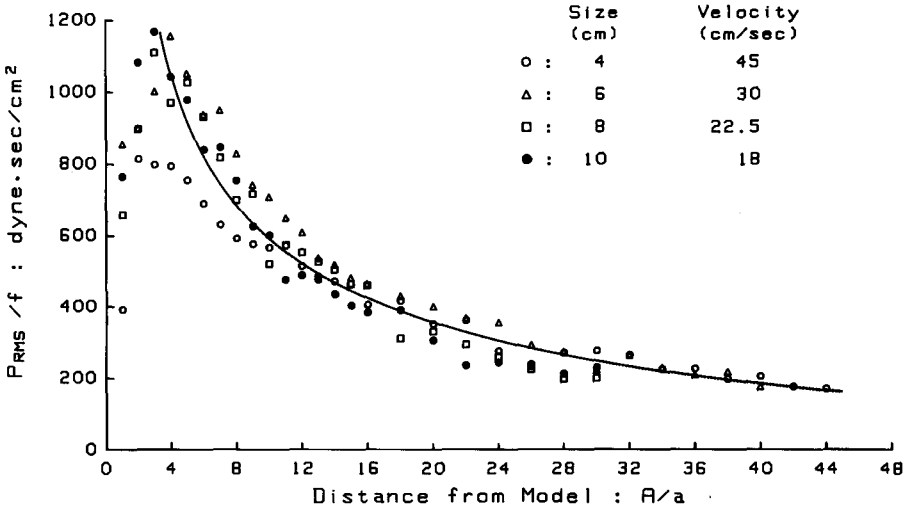

Fig. 3. The distributions of the parameter P_{RMS}/f along the central line ($B/a=0$) under the same Reynolds number 1.5×10^4, where P_{RMS} is the root mean square value of the sideward pressure of eddy, f, the unchangeable dominant freqency.

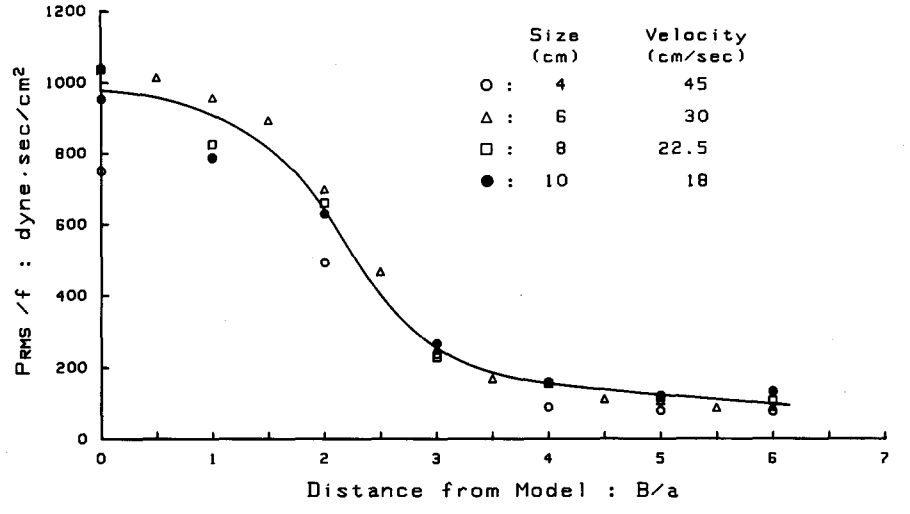

Fig. 4. The distributions of the parameter P_{RMS}/f along the cross line ($A/a=5$) under the same Reynolds number 1.5×10^4.

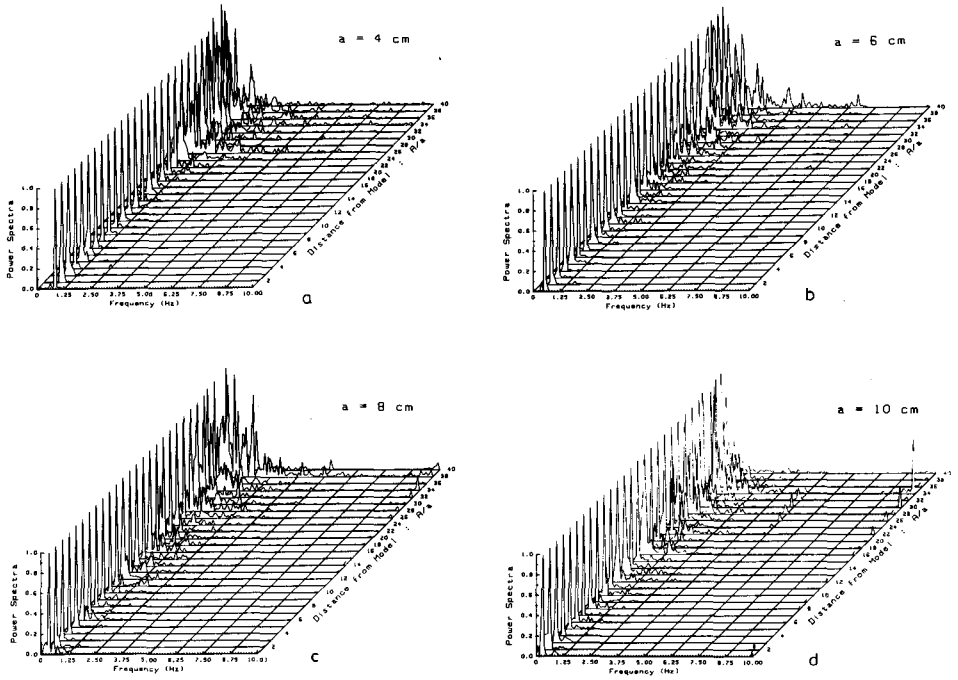

Fig. 5(a-d). The dominant freqency of eddies along the central line ($B/a=0$) under different Reynolds numbers with the same flow speed of 30 cm/sec.

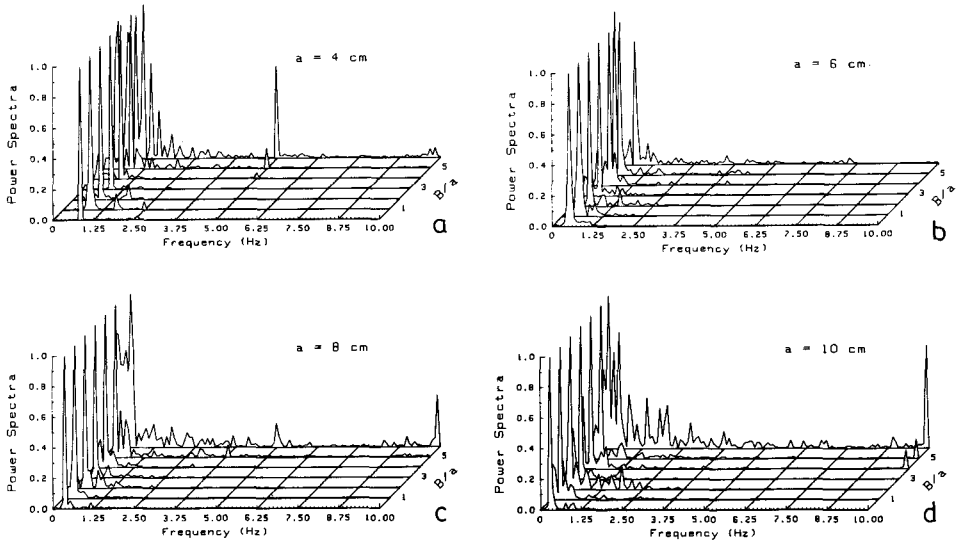

Fig. 6(a-d). The dominant freqency of eddies along the cross line ($A/a=5$) under different Reynolds numbers with the same flow speed of 30 cm/sec.

were almost geometrically similar, and that the eddy first developed and then was attenuated at approximately the point where $A/a=3$. This distance may be called the range of eddy development. From the power spectra and distributions it was found that the unchangeable dominant frequency became unstable at certain measuring points, and at those points the values of P_{RMS}/f were different. The value of P_{RMS}/f was greater at the central line than the cross line ($A/a=5$). This showed that a turbulent eddy area having no stable frequency existed.

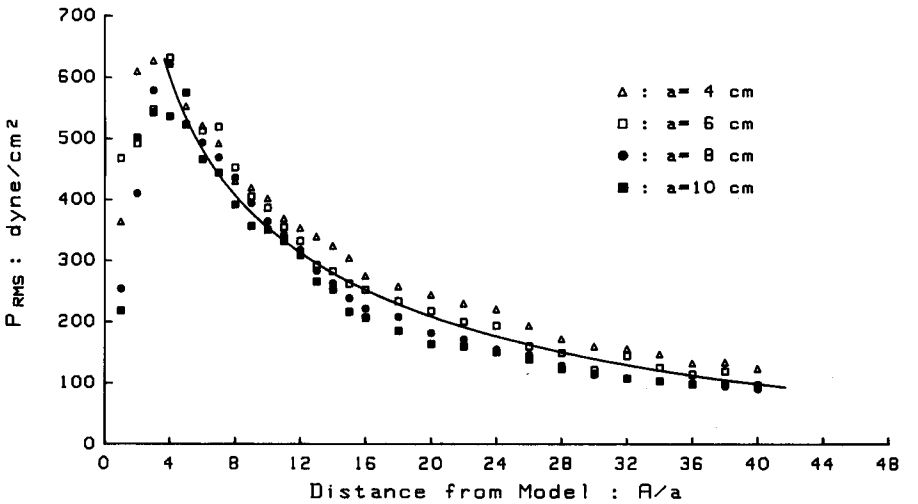

Fig. 7. The distributions of the P_{RMS} (root mean square value of the sideward pressure) along the central line ($B/a=0$) at the same flow speed of 30 cm/sec.

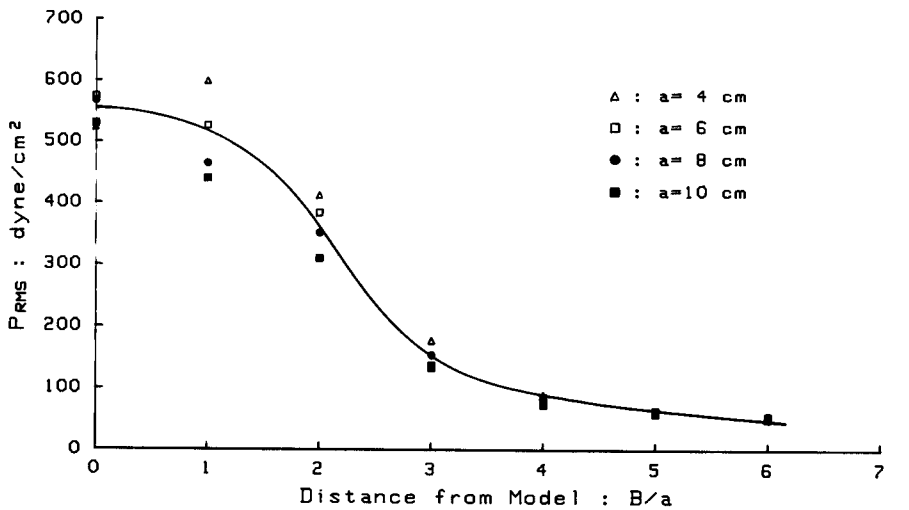

Fig. 8. The distributions of the P_{RMS} (root mean square value of the sideward pressure) along the cross line ($A/a=5$) under the same flow speed of 30 cm/sec.

The power spectra at the measuring points along the central line are shown in Fig. 5(a-d) for models with the same flow speed but different Reynolds numbers ranging from 1.0×10^4 to 2.5×10^4. Fig. 6(a-d) shows the power spectra at the side area. Results show that for all sizes the backward range of the eddy area having an unchangeable dominant frequency was the same, about 34~36 times the model size. The sideward range was about 5 times. The unchangeable dominant frequency was 0.86 Hz for the model of 4.0 cm, 0.55 Hz for 6.0 cm, 0.39 Hz for 8.0 cm and 0.31 Hz

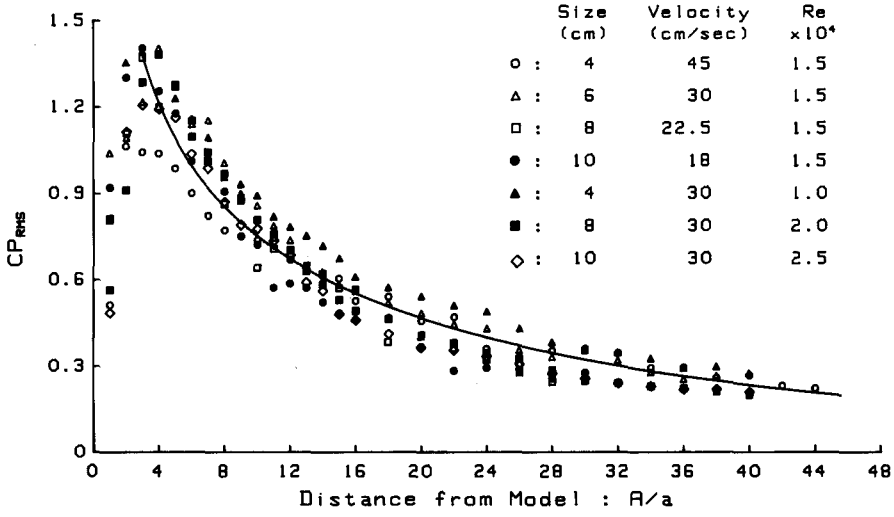

Fig. 9. The distributions of the non-dimensional parameter CP_{RMS} along the central line ($B/a=0$) for the different Reynolds numbers of 1.0×10^4~2.5×10^4.

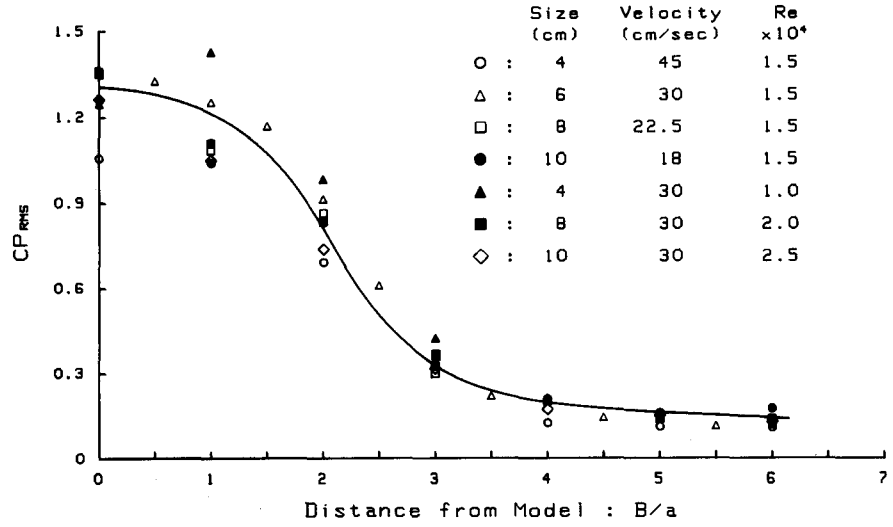

Fig. 10. The distributions of the non-dimensional parameter CP_{RMS} along the cross line ($A/a=5$) for the different Reynolds numbers of 1.0×10^4~2.5×10^4.

for 10.0 cm. The values of P_{RMS} along the central line and side area are shown in Fig. 7 and Fig. 8. The distributions of P_{RMS} were geometrically similar. The range of eddy development was at about the point where $A/a=3$. The turbulent eddy area also existed after the unchangeable dominant frequency became unstable.

Fig. 9 and Fig. 10 were obtained from Fig. 3, Fig. 4, Fig. 7 and Fig. 8 by the parameter CP_{RMS}. The distributions of the the values of the non-dimensional parameter were similar for the models under the different Reynolds numbers of $1.0\times 10^4 \sim 2.5\times 10^4$.

Discussions

The experimental results have shown the degree of similarity of the eddy area expressed by the parameter P_{RMS}/f for the same Reynolds number, and the parameter P_{RMS} for the same flow speed. The assumption and the previously derived Equations (6) and (8) are verified by these experimental results. Also, the non-dimensional parameter CP_{RMS} can be used to estimate the eddy area behind the models under conditions of both the same and different Reynolds numbers of $1.0\times 10^4 \sim 2.5\times 10^4$.

On the other hand, the eddy area can be divided into two parts: the effective eddy area and turbulent eddy area. It can be said that the effective eddy area has an unchangeable dominant frequency and that the energy concentrated on the dominant frequency is greater than on the other frequencies in the power spectrum of eddy; the turbulent eddy area has no such unchangeable dominant frerqency but the root mean square value of the sideward pressure of eddy is greater than that of the noise of the measuring background. The effective eddy area is almost the same for models with the same flow speed. This means that the effective eddy areas are also similar, although the dominant frequencies are different. The turbulent eddy areas can be determined by comparing the distributions of the P_{RMS} with the background noise levels. Because the eddy behind the models was measured along only two series of measuring points in this experiment, the effective and turbulent eddy areas remain to be determined in a future experiment.

Since the distributions of the P_{RMS} under the same flow speed are almost the same for models with the same shape but different size, under the same environmental conditions, the basic shape of the components in artificial reef structures will tend to increase or decrease the sideward pressure, and the basic size will tend to create a higher or lower frequency and to expand or narrow the eddy areas. Generally speaking, if flow speed is held constant, the frequency of the eddy is determined by the size of the components, while the sideward pressure is determined by the basic shape of the components. This suggests that the artificial reef structure could be designed more economically by considering the environmental conditions along with the properties of the eddy area behind the components. Also, the artificial reef structure can be made more effective if the reactions of fishes and other organisms to the eddy become well known.

References

Artificial Reef Comprehensive Research Association (in Japan) (1976). A review of artificial fishreef

research-I: primary subjects of artificial fishreef study. *Suisan Zoyoshoku Sosho* **26**, 9-39 (In Japanese).

Bohnsack, J.A. and Sutherland, D.J. (1985). Artificial research: a review with recommedations for future priorities. *Bull. Amer. Mar. Sci.* **37**, 11-39.

Kageyama, Y., Osaka, H., and Yamada, H. (1980). Flow visualization around the perforated cubic artificial fishreef-model by water tunnel testing. *Fisheries Engineering. Jap.* **17**, 1-10. (In Japanese).

Matsumi, Y. and Seyama, A. (1985). Flow pattern around a system of fish aggregation device. *Proc. of 32th Jap. Conf. on Coastal Eng.*, 652-656. (In Japanese).

Sakuta, H., Sakuta, M., Watanabe, K., and Onishi, H. (1981). Fundamental study of hydrodynamic characteristics of artificial reef model. *Fisheries Engineering. Jap.* **18**, 7-19. (In Japanese with English Abstract)

Sakuta, M., Kuroki, H., Takagi, G., Kawaguchi S., and Fukuda, H. (1982). Experimental study of hydrodynamic characteristics of large-scale artificial reefs: influenced areas of artificial reefs. *Proc. of the Academic Lecture Meeting in the Dep. of Sci. and Eng. of Jap. Univ.*, 53-55. (In Japanese)

Sato, O. (1977). Several problems about artificial reefs. *Coastal Oceanograghy Study Note.* **14**, 88-100. (In Japanese)

Sawaragi, T. and Matsumi, Y. (1981). Characteristics of the flow pattern behind fish aggregation device. *Proc. of 28th Jap. Conf. on Coastal Eng.*, 387-391. (In Japanese).

Sawaragi, T., Matsumi, Y. Hayashi, K. (1984). Numerical simulation of flow pattern around a fish aggregation device. *Coastal Eng. in Jap.*, **27**, 109-118.

Wang, C.H. and Sato, O. (1986). Hydrodynamic characteristics in simplified components of artificial reef structures. *Bull. Fac. Fish. Hokkaido Univ.* **37**, 190-206.